A NOVEL IMAGE CODING SCHEME BY USING TWO-CHANNEL COMPLEX-VALUED FILTER BANKS

Seisuke Kyochi, Yuichi Tanaka, and Masaaki Ikehara

Department of Electronics and Electrical Engineering, Keio University
3-14-1 Hiyoshi Kohoku, Yokohama Kanagawa 223-8522, Japan
Phone: +81-45-566-1463
Email: kyochi@tkhm.elec.keio.ac.jp

ABSTRACT

A novel image coding scheme by using two-channel complex-valued filter banks (CFBs) is proposed in this paper. Up to now, most of the image coding schemes have used real-valued filter banks (RFBs). In other words, there are no efficient image coding framework using CFBs since the amount of samples transformed by CFBs is twice as much as that of RFBs. However, CFBs are expected to have better frequency characteristics than RFBs, since CFBs have more design parameters than that of RFBs. Thus, if the problem is solved, CFBs could be efficient for image coding. In this paper, a new algorithm which can preserve the amount of information when CFBs are applied to image coding is introduced. It is shown that the proposed image coding scheme using CFBs is superior to conventional real-valued wavelet-based image coding.

1. INTRODUCTION

Recently, multirate filter banks (FBs) and wavelets have been extensively studied and found their applications in image compression. Fig. 1 shows an M-channel maximally decimated FB, where $H_k(z)$ and $F_k(z)$ are the k-th (for $k = 0, \cdots, M-1$) analysis and synthesis filters, respectively. Fig. 2 also shows its polyphase representation. The analysis and synthesis filters are represented by using the polyphase matrices $\mathbf{E}(z)$ and $\mathbf{R}(z)$ as follows:

$$\begin{aligned} [H_0(z)\, H_1(z) \cdots H_{M-1}(z)]^T &= \mathbf{E}(z^M)\mathbf{e}(z)^T \\ [F_0(z)\, F_1(z) \cdots F_{M-1}(z)] &= \mathbf{e}(z)\mathbf{R}(z^M) \\ \mathbf{e}(z) &= \left[1\; z^{-1} \cdots z^{-(M-1)}\right] \end{aligned} \tag{1}$$

A FBs is perfect reconstruction if and only if $\mathbf{E}(z)\mathbf{R}(z) = z^{-n}\mathbf{I}$, where $\mathbf{I}$ is an identity matrix and n is a natural number. FBs are usually designed and implemented by a lattice structure [1]. A lattice structure is derived from the factorization of the polyphase matrix.

There are some image coding standards such as JPEG [2] and JPEG2000 [3]. Discrete cosine transform (DCT) and discrete wavelet transform (DWT) are employed for JPEG and JPEG2000, respectively. In these days, various and effective FBs for image coding have been proposed. The lapped orthogonal transform (LOT) [4] and the generalized LOT (GenLOT) [5] are important examples of those classes of FBs. It is well-known that the FBs can reduce the blocking artifact which is the main disadvantage of the DCT. Most of the FBs for image coding proposed until now are real-valued FBs (RFBs).

Complex-valued FBs (CFBs) have received much interests and been studied in recent years. In [6] lattice structures

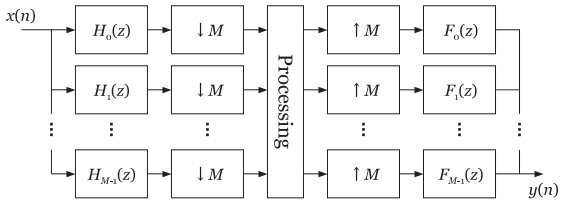

Figure 1: An M-channel FB.

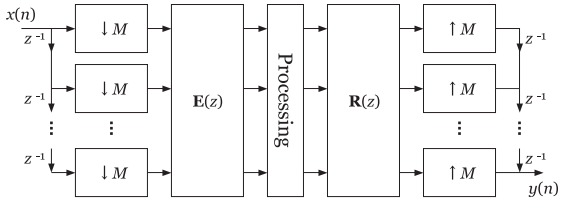

Figure 2: A polyphase structure of FB.

of M-channel complex-valued linear-phase paraunitary FBs (CLPPUFBs) and complex-valued symmetry-antisymmetry PUFBs (CSAPUFBs) with their filter lengths are $\alpha_k M + \beta_k$, where M, k, α_k and β_k are nutural number such that $M \geq 3$, $0 \leq k \leq M-1$, $0 \leq \alpha_m \leq K$ and $0 \leq \beta_k \leq M-1$, have been proposed. In the case of $M = 2$, it is well-known that there is no two-channel CLPPUFB except for its filter lengths of 2 [7]. In contrast, two-channel CSAPUFBs whose filter lengths are more than 2 exist [8].

In addition to these types of FBs, an another type of FBs has been proposed [9]. This class of FBs is called two-channel complex-valued linear-phase pseudo-orthogonal FBs (CLPPOFBs). The FBs satisfy the orthogonal property partially. Based on the pseudo-orthogonality, CLPFBs can be designed with filter lengths are more than 2.

There are several applications of CFBs, for example complex-valued signal processing, such as radar signals and QAM modulated signals , communication systems, audio processing, image denoising, and so on [10]-[14]. However, there is no efficient application of CFB for image coding since the amount of information of output signals doubles when CFBs are applied to real-valued signals. However, it is expected that CFBs have better performances than RFBs, since CFBs have more design parameters than that of RFBs. Therefore, if CFBs can preserve the amount of information, an image coding scheme using CFB has a potential to have better performance than the conventional real-valued image

coding method.

This paper is organized as follows. In section 2, we will review the conventional lattice structures of CFBs. In section 3, a novel image coding scheme by using CFBs is described. Finally, it is shown that proposed image coding scheme is superior to the wavelet-based image coding by the simulation in section 4.

Notations: $\mathbb{R}$ and $\mathbb{C}$ denote the set of real numbers and complex numbers, respectively. Bold faced letters indicate vectors and matrices. $\mathbf{I}$ and $\mathbf{J}$ are the identity and reversal identity matrix, respectively. $\overline{z}$ denotes the complex conjugate of z. $\mathbf{\Lambda}(z) := \begin{bmatrix} 1 & 0 \\ 0 & z^{-1} \end{bmatrix}$. The superscript $*$, T, and H denote the complex conjugated, the transpose and the complex conjugated transpose, respectively.

In the following section, FBs are always considered as the two-channel case.

2. REVIEW

2.1 CFBs

2.1.1 CPUFBs

A two-channel CFB is a complex-valued paraunitary FB (CPUFB) if and only if its analysis polyphase matrix $\mathbf{E}(z)$ satisfies the condition $\mathbf{E}(z)\mathbf{E}^H(z^{-1}) = \mathbf{I}$. Two-channel CPUFBs can be designed by the following lattice structure [1].

$$\mathbf{E}(z) = \mathbf{V}_N\mathbf{\Lambda}(z)\mathbf{V}_{N-2}\mathbf{\Lambda}(z)\dots\mathbf{V}_1\mathbf{\Lambda}(z)\mathbf{V}_0, \qquad (2)$$

where $\mathbf{V}_k$ $(0 \le k \le N)$ are $\mathbf{V}_k = \mathbf{X}_k\mathbf{\Theta}_k\mathbf{Y}_k$, and $\mathbf{X}_k, \mathbf{Y}_k$, and $\mathbf{\Theta}_k$ are

$$\mathbf{X}_k = \begin{bmatrix} \cos\theta_{X_k} & \sin\theta_{X_k} \\ -\sin\theta_{X_k} & \cos\theta_{X_k} \end{bmatrix}, \quad \mathbf{Y}_k = \begin{bmatrix} \cos\theta_{Y_k} & \sin\theta_{Y_k} \\ -\sin\theta_{Y_k} & \cos\theta_{Y_k} \end{bmatrix},$$

$$\mathbf{\Theta}_k = diag(e^{j\theta_k}, e^{j\theta_{k+1}}), \quad (\theta_{X_k}, \theta_{X_k}, \theta_k, \theta_{k+1} \in \mathbb{R})$$

respectively. Obviously, each of the building blocks has 4 design parameters.

2.1.2 CLPFBs

A two-channel CFB is complex-valued linear-phase FB (CLPFB) if and only if its analysis polyphase matrix $\mathbf{E}(z)$ satisfies $\mathbf{E}(z) = diag(1,-1)\mathbf{E}^*(z^{-1})\mathbf{J}$. Two-channel CLPFBs can be designed by the following lattice structure [1].

$$\mathbf{E}(z) = \mathbf{S}_N\mathbf{\Lambda}(z)\mathbf{S}_{N-2}\mathbf{\Lambda}(z)\dots\mathbf{S}_1\mathbf{\Lambda}(z)\mathbf{S}_0, \qquad (3)$$

where $\mathbf{S}_k$ $(0 \le k \le N)$ are $\mathbf{S}_k = \begin{bmatrix} a & b \\ \overline{b} & \overline{a} \end{bmatrix}$ Each building block of a CLPFB has 2 design parameters.

2.1.3 CSAPUFBs

It is well-known that CLPPUFBs with their filter lengths more than 2 can not be designed [7]. In other words, it is impossible to design CPUFBs whose filters are hermitian symmetric or hermitian antisymmetric and have a length of more than 2. However CPUFBs whose filters are only symmetric or antisymmetric (CSAPUFBs) and the filter length more than 2 can be designed by the following lattice structure [8].

$$\mathbf{E}(z) = \frac{\sqrt{2}}{2^N}\begin{bmatrix} v_{N-1} & 0 \\ 0 & v_N \end{bmatrix}\prod_{k=N-2}^{0}\left\{\begin{bmatrix} 1 & 1 \\ 1 & -1 \end{bmatrix}\right.$$
$$\left.\begin{bmatrix} 1 & 0 \\ 0 & z^{-1} \end{bmatrix}\begin{bmatrix} 1 & 1 \\ 1 & -1 \end{bmatrix}\begin{bmatrix} 1 & 0 \\ 0 & v_k \end{bmatrix}\right\}\begin{bmatrix} 1 & 1 \\ 1 & -1 \end{bmatrix}, \qquad (4)$$

where $v_k = e^{j\theta_k}$ $(\theta_k \in \mathbb{R}, 0 \le k \le N)$. Each of the building blocks of CSAPUFB has 1 design parameter.

Since CSAPUFBs impose symmetry and antisymmetry properties on their filters, their frequency responses are symmetric. Moreover it is known that, for any CSAPUFB, there exists a RFB with identical frequency responses [7].

2.1.4 CLPPOFBs

PU and LP properties are important for FBs. One advantage of PUFBs is that FBs can be designed easier than biorthogonal ones. On the other hand, the advantage of LPFBs is that the symmetric extension can be applied at boundaries of signals. Hence, FBs satisfying both PU and LP properties are highly desired. Unfortunately, as mentioned previously, it is impossible to construct two-channel CLPPUFBs whose filter lengths are more than 2 [7].

Recently, a new concept called pseudo-orthogonality has been proposed [9]. A two-channel CFB is a complex-valued pseudo-orthogonal FB (CPOFB) if and only if its analysis polyphase matrix $\mathbf{E}(z)$ satisfies the condition $\mathbf{E}(z)\mathbf{E}^T(z^{-1}) = \mathbf{I}$. If a FB is CPOFB, then its synthesis polyphase matrix $\mathbf{R}(z)$ can be designed as the transpose version (not conjugated transposed) of $\mathbf{E}(z)$. Therefore, pseudo-orthogonality inherits an advantage of the PU property. Furthermore, it is shown that CPOFBs can have LP filters whose lengths are more than 2. The class of FBs is called CLPPOFB.

Two-channel CLPPOFBs can be designed by the following lattice structure [9].

$$\mathbf{E}(z) = \frac{1}{\sqrt{2}}\begin{bmatrix} 1 & 1 \\ 1 & -1 \end{bmatrix}\mathbf{V}_N\mathbf{\Lambda}(z)\mathbf{V}_{N-1}\cdots\mathbf{V}_1\mathbf{\Lambda}(z)\mathbf{V}_0 \qquad (5)$$

where $\mathbf{V}_k$ is

$$\mathbf{V}_k = \frac{1}{\sqrt{s_k^2 - t_k^2}}\begin{bmatrix} s_k & jt_k \\ -jt_k & s_k \end{bmatrix} \quad (s_k \ne t_k) \qquad (6)$$

where s_k and t_k are real number.

2.2 Evaluation of the CFBs performance

In this section, we compare the CFB's performance to the RFB's one. As mentioned previously, it can be considered that CFBs could have better frequency characteristics than RFBs since RFBs form a subclass of CFBs. Therefore, for every evaluation criteria of the FB's performance, we could choose an optimal FB in complex number field.

Here, we compare the performance between RFBs and CFBs. The FBs used for the comparison are two-channel real-valued and complex-valued PUFBs (RPUFBs and CPUFBs). The lattice structure of CPUFBs is described in (2) and RPUFB is represented as follows [1].

$$\mathbf{E}(z) = \mathbf{R}_N\mathbf{\Lambda}(z)\mathbf{R}_{N-1}\mathbf{\Lambda}(z)\dots\mathbf{R}_1\mathbf{\Lambda}(z)\mathbf{R}_0, \qquad (7)$$

Table 1: Result of Energy Error

	K=6	K=8	K=10
RPUFB	144.162	137.698	137.088
CPUFB	24.314	23.690	23.549
	K=12	K=14	K=16
RPUFB	137.028	137.005	137.001
CPUFB	23.516	23.508	23.506

where $\mathbf{R}_k(z) = \begin{bmatrix} \cos\theta_k & \sin\theta_k \\ -\sin\theta_k & \cos\theta_k \end{bmatrix}$ $(0 \le k \le N, \theta_k \in \mathbb{R})$. The criteria used in the simulation is the following equation.

$$\begin{aligned} \Phi_{EE} &= \sum_{i=0}^{1} (E_{pass}^{(i)} + E_{stop}^{(i)}), \\ E_{pass}^{(i)} &= \int_{\Omega_{i,p}} (1 - |H_i(\omega)|)^2 d\omega, \\ E_{stop}^{(i)} &= \int_{\Omega_{i,s}} |H_i(\omega)|^2 d\omega, \end{aligned} \tag{8}$$

where $i \in \{0,1\}$, $H_0(\omega)$ and $H_1(\omega)$ are transfer functions of the lowpass and highpass filter, $E_{pass}^{(0)}, E_{stop}^{(0)}, E_{pass}^{(1)}$ and $E_{stop}^{(1)}$ are the passband and stopband energy error of the lowpass and highpass filter, respectively. Both types of FBs are optimized for some filter lengths to minimize Φ_{EE} and the result is shown in Table 1. This result shows that CFBs can be designed to have better performance than RFBs.

3. PROPOSED ALGORITHM

In this section, the image coding algorithm by using CFBs which can preserve the amount of information is proposed. The algorithm consists of five stages. Fig. 3 indicates the entire proposed algorithm.

Stage 1. Convert the original image to a half-size complex-valued image.

In this stage, the original image is transformed to a complex-valued image. This flow is shown in Fig. 3, where $E_0(z)$ and $E_1(z)$ are analysis lowpass and highpass filters of two-channel RFBs, respectively.

First, the original image is transformed by $E_0(z)$ and $E_1(z)$ horizontally and decimated by 2. Then, the lowpass coefficients are added to the highpass coefficients multiplied by $j = \sqrt{-1}$

In z-domain, This process can be represented as follows.

$$\begin{aligned} Y(z) =& E_0(z)X(z) + j * E_1(z)X(z) \\ =& \{E_0(z) + j * E_1(z)\}X(z) \\ =& H(z)X(z) \end{aligned} \tag{9}$$

where $H(z) = E_0(z) + j * E_1(z)$ and $X(z)$ and $Y(z)$ are the z-transforms of the original image and the transformed complex-valued one, respectively. From (9), it can be regarded that the original image is transformed by $H(z)$. Since real and imaginary parts of a complex number are independent of each other, the original image can be reconstructed from the complex-valued image without loss of information. Note that the original image and the half size complex-valued image have obviously the same amount of information. Hence, the proposed algorithm can preserve the amount of information.

Stage 2. Transform by the CFBs.

In this stage, the complex-valued image is transformed by a CFB vertically and horizontally. $H_0(z)$ and $H_1(z)$ in Fig. 3 are the analysis lowpass and highpass filters of the CFB, respectively.

Stage 3. Transform by DWT.

LL subband coefficients output by the CFB in the previous stage are transformed by the 9/7-tap Daubechies wavelet filters recursively. $W_0(z)$ and $W_1(z)$ in Fig. 3 are the analysis lowpass and highpass filter of the 9/7-tap Daubechies wavelet filters.

Stage 4. Replace the coefficients.

In this stage, the output complex-valued coefficients are divided into real and imaginary parts. Then, as in Fig. 3, the coefficients are replaced in each of LL · LH · HL · HH subbands.

Stage 5. Code all the subband coefficients.

All the coefficients replaced in the previous stage are coded in this stage. Note that all the replaced coefficients are real number and the same amount of information of the original image. In this paper, we adopt EZW based on intraband partitioning (EZW-IP) [15] for coding.

4. SIMULATION

In this section, our proposed image coding scheme is compared with the 9/7-tap Daubechies wavelet transform as in JPEG2000.

In stage 1, we adopted the 9/7-tap Daubechies wavelet filters as $E_0(z)$ and $E_1(z)$. In stage 2, we adopted a CPUFB and CLPPOFB as the CFBs. CSAPUFBs are not suited for the proposed image coding scheme since their performance is regarded as that in a RFB, mentioned in Sec. 2.1.3. Therefore, CSAPUFBs are not chosen in this simulation. Both of the CPUFB and CLPPOFB are designed based on (2) and (5), respectively. Especially, the building blocks of CLPPOFB in (6) are optimized with the following building blocks:

$$V_k = \begin{bmatrix} \cos\theta_k & -j\sin\theta_k \\ j\sin\theta_k & \cos\theta_k \end{bmatrix} \quad (\theta_k \in \mathbb{R}). \tag{10}$$

The filter lengths are set to 16 (Order-7) and the number of design parameters are 28 for CPUFB and 7 for CLPPOFB.

Three cost functions are used as the evaluation criteria. The first is the passband and stopband energy error Φ_{EE} in (8). The second is the DC leakage Φ_{DC} defined as follows:

$$\Phi_{DC} = \sum_{k=0}^{1} \sum_{i=0}^{N-1} h_k(i) \tag{11}$$

The third is the energy compaction Φ_{EC}. This is the energy ratio defined as follows:

$$\Phi_{EC} = \frac{\sum_{k \in all\ subband} |C_k|^2}{\sum_{k \in LL\ subband} |\Re\{C_k\}|^2}, \tag{12}$$

where $\{C_k\}$ is the output signal of the image transformed by the CFB and $\Re\{C_k\}$ is the real part of each C_k. Φ_{EC} is used for the energy compaction. In this simulation, we adopted *Barbara* as a reference image.

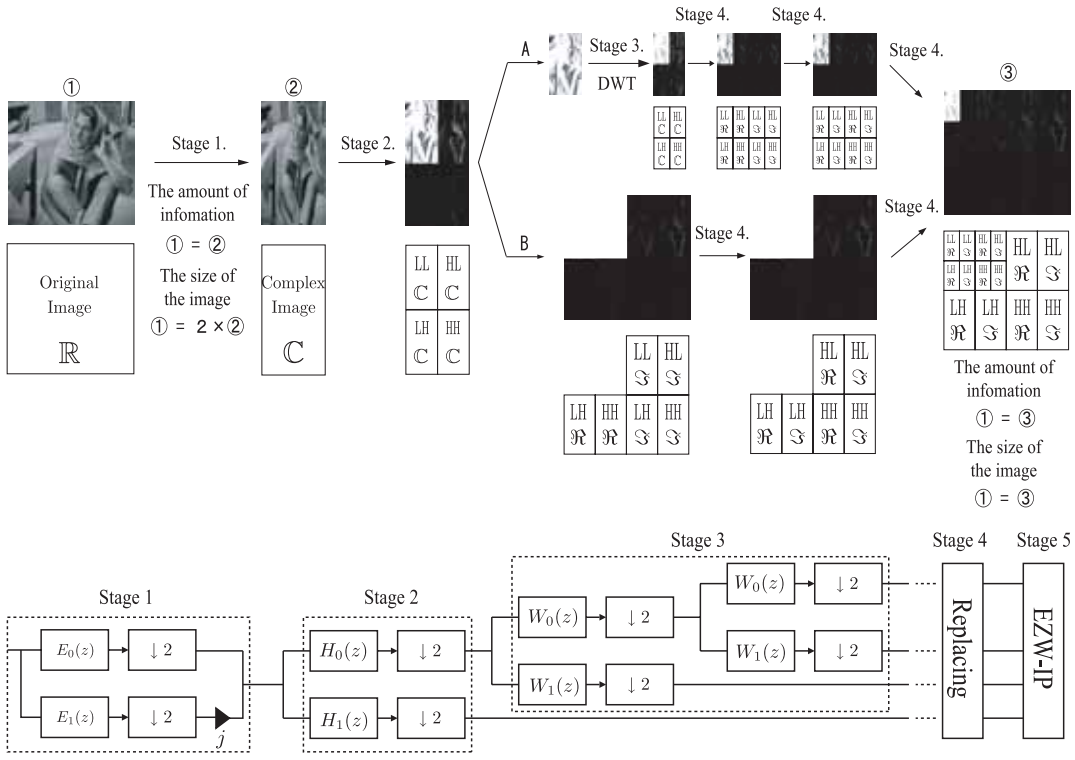

Figure 3: Outline of the proposed algorithm

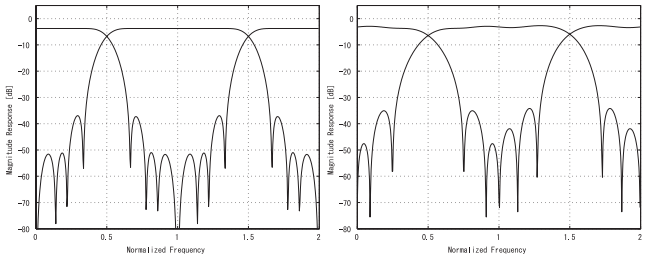

(a)CPUFB (b)CLPPOFB

Figure 4: Frequency responses

Table 2: Image coding results

		9/7	CPUFB	CLPPOFB
Image	PSNR [db]	Bit rate [bpp]		
Barbara	34.915	1.000	0.941	0.955
Bridge	28.744	1.000	1.000	0.995
Baboon	27.592	1.000	0.996	0.988
Finger	29.045	1.000	0.913	1.000
Tank	35.126	1.000	0.957	0.954
Car and Apc	35.746	1.000	0.965	0.972
Washsat	34.633	1.000	0.999	1.001
Goldhill	35.126	1.000	1.010	0.991

Finally we defined Φ as a weighted linear combination of Φ_{EE}, Φ_{DC} and Φ_{EC}:

$$\Phi = \omega_{EE}\Phi_{EE} + \omega_{DC}\Phi_{DC} + \omega_{EC}\Phi_{EC} \qquad (13)$$

and minimized. The frequency responses of the designed CPUFB and CLPPOFB are depicted in Fig. 4. In the stage 3, the 9/7-tap Daubechies wavelet transform is applied to LL subband coefficients 5 times recursively. Meanwhile, for fair comparison, an image is transformed by the 9/7-tap Daubechies wavelet transform 6 times recursively for the real-valued transform.

We compare the proposed image coding scheme to the conventional wavelet-based image coding in the bit rate, under the same PSNR. For that, we first applied the 9/7-tap Daubechies wavelet filters to the original images, coded at 1 [bpp], and calculated the PSNR for each image. Then we adopted the CPUFB and CLPPOFB to the original images and coded so that the resulting PSNRs are equal to those of the 9/7-tap Daubechies wavelet filters. The results are shown in Table 2 and compressed image examples are shown in Fig. 5. Table 2 and Fig. 5 show that the proposed image coding scheme can realize the same image quality of the conventional wavelet-based image coding at the same or less bit rate. Therefore the proposed image coding scheme using CFBs superior to the conventionalwavelet-based image coding. Furthermore, it can be seen that CLPPOFB realize almost the same image quality of the CPUFB using four times less design parameters. Moreover CLPPOFBs have the LP property which is useful for image coding. Hence, CLPPOFBs are more suitable for the proposed image coding scheme than CPUFBs.

5. CONCLUSION

In this paper, we introduced a novel image coding scheme using CFBs. The proposed technique can preserve the amount

(a)9/7 wavelet (b)CPUFB (c)CLPPOFB

Figure 5: Result Image

of information of the original image even if CFBs are applied for image coding. Hence, the proposed method can solve the problem, which the amount of information of the image is doubled due to complex coefficients of CFBs.

In the simulation, our proposed image coding scheme obtains better results than the conventional real-valued wavelet-based image coding. As a result, it is shown that our proposed method has better performance than that of conventional one. Moreover, we compared CPUFBs and CLPPOFBs for image coding. Each building block in a CLPPOFB has four times less design parameters than that of a CPUFB. Nevertheless, CLPPOFBs can realize comparable performance to CPUFBs since CLPPOFBs have the LP property and can apply the symmetric extension at the boundary of the image. Therefore, CLPPOFBs are more suitable for the proposed image coding than CPUFBs.

REFERENCES

[1] P. P. Vaidyanathan, *Multirate Systems and Filter Banks*. Englewood Cliffs, NJ: Prentice-Hall, 1993.

[2] K. R. Rao and P.Yip, "Discrete Cosine Transform: Algorithms, Advantages, Applications," Academic Press, 1990.

[3] A. Skodras, C. Christopoulis and T. Ebrahimi, "The JPEG2000 Still Image Compression Standard," *IEEE Trans. Signal Process. Mag*., vol. 18, no. 5, pp. 36-58, Sept. 2001.

[4] E. S.Malvar and D. H. Staelin, "The LOT: Transform Coding Without Blocking Effects," *IEEE Trans. Signal Process*., vol. 37, no. 4, Apr. 1989.

[5] R. L. de Queiroz, Troung Q. Nguyen, and K. R. Rao, "The GenLOT: Generalized Linear-Phase Lapped Orthogonal Transform," *IEEE Trans. Signal Process*., vol. 44, no. 3, pp. 497–507, Mar. 1996.

[6] X. Q. Gao, T. Q. Nguyen, and G. Strang, "Theory and lattice structure of complex paraunitary filterbanks with filters of (hermitian-) symmetry/antisymmetry properties," *IEEE Trans. Signal Process*., vol. 49, no. 5, pp. 1028–1043, May, 2001.

[7] X.-P. Zhang, M. D. Desai, and Y.-N. Peng, "Orthogonal complex filter banks and wavelets: some properties and design," *IEEE Trans. Signal Process*., vol. 47, no. 4, pp. 1039–1048, Apr, 1999.

[8] X. Q. Gao, T. Q. Nguyen, and G. Strang, "A study of two-channel complex-valued filterbanks and wavelets with orthogonality and symmetry properties," *IEEE Trans. Signal Process*., vol. 50, no. 4, pp. 824–833, Apr, 2002.

[9] S. Kyochi, Y. Tanaka, and M. Ikehara, "Theory and Design of Two-Channel Complex Linear-Phase Pseudo-Orthogonal Filterbanks," in Proc. Int Conf. Acoustics, Speech, and Signal Process., vol 3. 245–248, May, 2006.

[10] G. Wei and S Wu, "Denoising radar signals using complex wavelet," in Proc. Int Sym. Signal Process. and Its Applications, vol 1. 341–344, July, 2003.

[11] T. K. Adhikary and V. U. Reddy, "Complex wavelet packets for multicarrier modulation," in Proc. Int Conf. Acoustics, Speech, and Signal Process., vol 3. 1821–1824, May, 1998.

[12] W. Lawton, "Minimax threshold for denoising complex signals with waveshrink," *IEEE Trans. Signal Process*., vol. 48, pp. 1821–1824, Apr, 2000.

[13] H. Malvar, "A modulated complex lapped transform and its applications to audio processing," in *Proc. IEEE ICASSP*., vol. 3, pp. 1421–1424, Mar, 1999.

[14] Ben Belzer, Jean-Marc Lina, and John Villasenor, "Complex, Linear-Phase Filters for Efficient Image Coding," *IEEE Trans. Signal Process*., vol. 43, no. 10, pp. 2425–2427, Oct, 1995.

[15] Z. Liu and L. J. Karam, "An efficient embedded zerotree wavelet image codec based on intraband partitioning," in Proc. Int Conf. Image Process., vol. 3, pp. 162–165, Sept, 2000.